KSCE Journal of Civil Engineering
Vol. 9, No. 2 / March 2005
pp. 161~169

Analysis of Flow Structure over Ogee-Spillway in Consideration of Scale and Roughness Effects by Using CFD Model

By Dae Geun Kim* and Jae Hyun Park**

Abstract

In this study, flow characteristics such as flowrate, water surfaces, crest pressures on the ogee-spillway, and vertical distributions of velocity and pressure in consideration of model scale and surface roughness effects are investigated in detail by using the commercial CFD model, FLOW-3D, which is widely verified and used in the field of spillway flow analysis. Numerical errors in the discharge flowrate, water surfaces, and crest pressures due to the surface roughness are insignificant if we just use a general roughness height of construction materials, and the scale effects of the model are in an acceptable error range if the length scale ratio is less than 100 or 200. The roughness and scale effects are more severe below h_m, where the maximum velocity occurs in perpendicular coordinate to the weir crest. The velocity of the prototype is larger than that of the scaled model below but the phenomena are contrary above h_m. Maximum velocity at any section slightly decreases as the surface roughness and the length scale ratio increase. The vertical location where maximum velocity occurs is located on a lower position as the upstream water head increases and the location almost linearly increases with the distance from the front of the spillway.

Keywords: *FLOW-3D, ogee-spillway, roughness effect, scale effect*

1. Introduction

The ogee-crested spillway's ability to pass flows efficiently and safely, when properly designed and constructed, with relatively good flow measuring capabilities, has enabled engineers to use it in a wide variety of situations as a water discharge structure (USACE, 1988; USBR, 1973). The ogee-crested spillway's performance attributes are due to its shape being derived from the lower surface of an aerated nappe flowing over a sharp-crested weir. The ogee shape results in near-atmospheric pressure over the crest section for a design head. At heads lower than the design head, the discharge is less because of crest resistance. At higher heads, the discharge is greater than an aerated sharp-crested weir because the negative crest pressure suctions more flow. Although much is understood about the general ogee shape and its flow characteristics, it is also understood that a deviation from the standard design parameters such as a change in upstream flow conditions, modified crest shape, or change in approach channel owing to local geometric properties can change the flow properties. For the analysis of the effects, physical models have been used extensively because a spillway is very important for the safety of dams. The disadvantages with the physical models are high costs and that it can take fairly long time to get the results. Also, errors due to scale effects may increases in severity as the ratio of prototype to model size increases. So, numerical modeling, even if it cannot be used for the final determination of the design, is valuable for obtaining a guide to correct details because computational cost is low relative to physical modeling.

In the past few years, several researchers have attempted to solve the flow over spillway with a variety of mathematical models and computational methods. The main difficulty of the problem is the flow transition from subcritical to supercritical flow. In addition, the discharge is unknown and must be solved as part of the solution. This is especially critical when the velocity head upstream from the spillway is a significant part of the total upstream head.

An early attempt of modeling spillway flow have used potential flow theory and mapping into the complex potential plane (Cassidy, 1965). A better convergence of Cassidy's solution was obtained by Ikegawa and Washizu (1973), Betts (1979), and Li *et al*. (1989) using linear finite elements and the variation principle. They were able to produce answers for the free surface and crest pressures and found agreement with experimental data. Guo *et al*. (1998) expanded on the potential flow theory by applying the analytical functional boundary value theory with the substitution of variables to derive nonsingular boundary integral equations. This method was applied successfully to spillways with a free drop. Assy (2000) used a stream function to analyze the irrotational flow over spillway crests. The approach is based on the finite difference method with a new representation of Neumann's problem on boundary points, and it gives positive results. The results are in agreement with those obtained by way of experiments. Unami *et al*. (1999) developed a numerical model using the finite element and finite-volume methods for the resolution of two dimensional free surface flow equations including air entrainment and applied it to the calculation of the flow in a spillway. The results prove that the model is valid as a primary analysis tool for the hydraulic design of spillways. Song and Zhou (1999) developed a numerical model that may be

*Member, Lecturer, Dept. of Civil Engineering, Mokpo National University, Korea (Corresponding Author, E-mail: kdg05@mokpo.ac.kr)
**Member, Assistant Professor, Dept. of Civil Engineering, Inje University, Korea

applied to analyze the 3D flow pattern of the tunnel or chute spillways, particularly the inlet geometry effect on flow condition. Olsen and Kjellesvig (1988) included viscous effects by numerically solving the Reynolds-averaged Navier-Stokes (RANS) equations, using the standard κ-ε equations to model turbulence. They showed excellent agreement for water surfaces and discharge coefficients. Recently, investigations of flow over ogee-spillways were carried out using a commercially available computational fluid dynamics program, FLOW-3D, which solves the RANS equations (Ho *et al*., 2001; Kim, 2003; Savage *et al*., 2001). They showed that there is reasonably good agreement between the physical and numerical models for both pressures and discharges. Especially, Kim (2003) investigated the scale effects of the physical model by using FLOW-3D. The results of numerical simulation on the series of scale models showed different flow discharges. Discharge and velocity of larger scale models has shown larger value than the smaller scale models.

Existing studies using CFD model mostly deal with the model's applicability to discharge flowrate, water surfaces, and crest pressures on the spillway. In this study, flow characteristics such as flowrate, water surfaces, crest pressures on the spillway, and vertical distributions of velocity and pressure in consideration of model scale and surface roughness effects are investigated in detail by using commercial CFD model, FLOW-3D, which is widely verified and used in the field of spillway flow analysis. The objective of this study is to investigate quantitatively the scale and roughness effects on the flow characteristics by analyzing the computational results.

2. Theoretical Background

2.1. Scaling and Roughness

A hydraulic model uses a scaled model for replicating flow patterns in many natural flow systems and for evaluating the performance of hydraulic structures. Shortcomings in models usually are termed scale effects of laboratory effects. Scale effects increase in severity as the ratio of prototype to model size increases or the number of physical processes to be replicated simultaneously increases. Laboratory effects arise because of limitations in space, model constructability, instrumentation, or measurement. Generally, steady nonuniform flow characteristics in open channel flow with hydraulic structures can be explained as a following relationship (ASCE, 2000).

$$S_w = \phi\left(S_o, \frac{k}{h}, \frac{V^2}{\sqrt{gh}}, \frac{Vh}{\nu}, \frac{\rho V^2 h}{\sigma}\right) \qquad (1)$$

where S_w is water surface slope, S_o is channel bottom slope, h is water depth, k is roughness height of solid boundary, V is flow velocity, g is gravitational acceleration, and ν, ρ, σ are dynamic viscosity, density, surface tension of water, respectively. Eq. (1) states that water surface profile is expressed as bottom slope, relative roughness height, Froude number, Reynolds number and Weber number. Similarity of variables in Eq. (1) between scaled model and prototype is maintained for the hydraulic model to properly replicate features of a complicated prototype flow situation.

Generally, geometric similarity (S_o) is achieved and experiments are carried out by using Froude number similarity in the hydraulic model on the open channel flow and hydraulic structures. Water is used to analyze the flow characteristics of scaled model, thus modeling accuracy is compromised because the properties of water are not scaled. So, a small scale model may causes a failure to simulate the forces attendant to fluid properties such as viscosity and surface tension, to exhibit different flow behavior than that of a prototype. Moreover, relative roughness height of the scaled model cannot be exactly reproduced because materials of experiment are limited.

Table 1. Approximate Values of Roughness Height, *k*

Materials	*k* (mm)
Concrete	0.100 ~ 3.000
Brass, Copper, Lead, Glass, Plastic	0.0015 ~ 0.007

Previous study on the scale limits of hydraulic models leads to some guidelines. The Bureau of Reclamation (1980) used length scale ratios of $L_r = 30{\sim}100$ for models of spillways on large dams. And model flow depths over a spillway crest should be at least 75 mm for the spillway's design operating range. The average roughness height for a given surface can be determined by experiments. Table 1 gives values of roughness height for several kinds of material which are used for construction of hydraulics structures and scaled models (Hager, 1999).

To determine quantitatively how scale and roughness effects influence the model results, it is possible to use a series of scale models with different surface roughness including prototype. But the hydraulic model experiments are expensive, time-consuming, and there are many difficulties in measuring the data in detail. Today, with the advance in computer technology and more efficient CFD codes, the flow behavior over ogee-spillways can be investigated numerically in a reasonable amount of time and cost.

2.2. Ogee-Spillway

Type 1 standard ogee-crested spillway (USACE, 1988) is depicted in Fig. 1 in which P is the weir height, H_d is the design head over the weir, H_o is the elevation head, and H_e is the total head including the velocity head, H_v. h_o is the water depth perpendicularly measured from the weir surface. The empirical equation for discharge is given by

$$Q = C \cdot L \cdot H_e^{1.5} \qquad (2)$$

where C = discharge coefficient and L_e = lateral crest length. Usually, Eq. (2) requires an additional energy equation and an

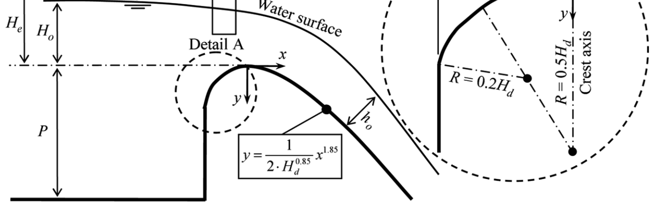

Fig. 1. Standard Ogee-crested Spillway Shape (Type 1)

iterative solution to determine the flowrate because the velocity head is not known until the flowrate is calculated. Because the velocity head is generally a small part of the total head, the equation converges to a solution after several iterations.

3. Numerical Methodologies

3.1. Governing Equations and Computational Scheme

The commercially available CFD package, FLOW-3D, uses the finite-volume approach to solve the RANS equations by the implementation of the Fractional Area/Volume Obstacle Representation (FAVOR) method to define an obstacle (Flow Science, 2002). The general governing RANS and continuity equations for incompressible flow, including the FAVOR variables, are given by

$$\frac{\partial}{\partial x_i}(u_i A_i) = 0 \tag{3}$$

$$\frac{\partial u_i}{\partial t} + \frac{1}{V_F}\left(u_j A_j \frac{\partial u_i}{\partial x_j}\right) = \frac{1}{\rho}\frac{\partial p}{\partial x_i} + g_i + f_i \tag{4}$$

where u_i represent the velocities in the x_i directions which are x, y, z-directions; t is time; A_i is fractional areas open to flow in the subscript directions; V_F is volume fraction of fluid in each cell; ρ is density; p is hydrostatic pressure; g_i is gravitational force in the subscript directions; f_i represents the Reynolds stresses for which a turbulence model is required for closure.

To numerically solve the rapidly varying flow over an ogee crest, it is important that the free surface is accurately tracked. In FLOW-3D, free surface is defined in terms of the volume of fluid (VOF) function which represents the volume of fraction occupied by the fluid.

A two-equation renormalized group theory models (RNG model) was used for turbulence closure. The RNG model is known to describe more accurately low intensity turbulence flows and flow having strong shear regions (Yakhot *et al*., 1992).

The flow region is subdivided into a mesh of fixed rectangular cells. With each cell there are associated local average values of all dependent variables. All variables are located at the centers of the cells except for velocities, which are located at cell faces (staggered grid arrangement). Curved obstacles, wall boundaries, or other geometric features are embedded in the mesh by defining the fractional face areas and fractional volumes of the cells that are open to flow.

3.2. Numerical Model Implementation

Two-dimensional numerical modeling (unit layer in y-direction) is carried out as shown in Fig. 2 in which z-direction replaces upward y-direction in Fig. 1 for the modeling convenience. Dimensions of modeling region are 7 H_d long and 3 H_d high. To speed up convergence to a steady state solution, a manual multi-grid method was implemented. The use of an initial coarse grid allowed an approximate water surface and flowrate to be quickly calculated. A sequential finer grid was then initialized by interpolating the previous calculated values onto the grid. Starting the new grid with the old values allowed the new solution to converge quicker. A final orthogonal grid in which Δx is 0.01 H_d to 0.14 H_d and Δz 0.01 H_d to 0.04 H_d is used. The fluid properties of 20°C water are used.

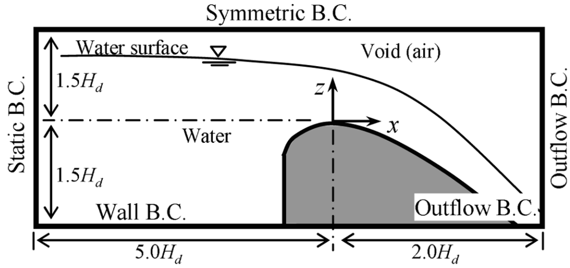

Fig. 2. Dimensions of Modeling Region and Boundary Conditions for the Modeling

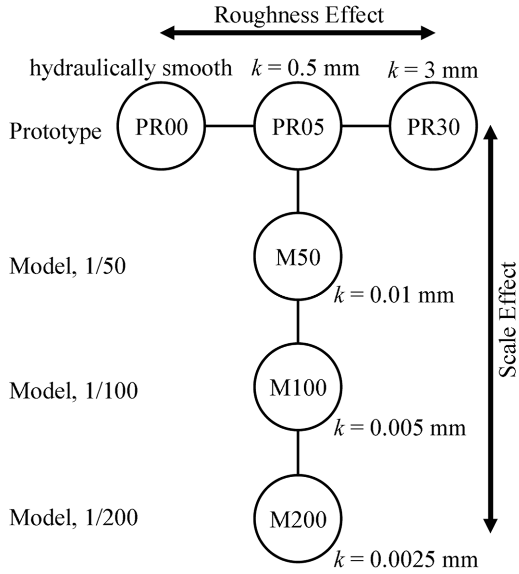

Fig. 3. Modeling Cases

To investigate the scaling and roughness effects, six cases as shown in Fig. 3 are adopted. Numerical modeling on the PR00, PR05, PR30 for the investigation of roughness effects and PR05, M50, M100, M200 for the investigation of scale effects are carried out. The prototype ogee-spillway is generally a concrete structure, so its roughness height is selected as 0.5 mm. For the analysis of roughness effects which are related to relative roughness height in Eq. (1), numerical modeling on the hydraulically smooth surface and 3.0 mm surface roughness height is carried out. For the analysis of scale effects which are related to Reynolds and Weber number in Eq. (1), numerical modeling on the 1/50, 1/100, and 1/200 scaled model is carried out. In the modeling of the scaled model, grid resolution is maintained like a modeling of the prototype. In this study, the surface tension effects are not considered, so only the viscosity effects lead to the scale effects.

3.3. Boundary Conditions

Boundary conditions of given flow are as shown in Fig. 2. The following boundary conditions were adopted: upstream hydrostatic pressure; downstream outflow; bottom upstream blocked by obstacle below (no slip); bottom downstream outflow; top symmetry (no influence in this case because of gravity). The ogee-crested obstacle boundary was modeled as a surface with no slip. With this configuration, the flow moves left to right between the no slip floor and weir and the atmospheric pressure boundary at the top. No slip is defined as zero tangential and

Table 2. Upstream Boundary Conditions and Modeling Time

Case		H_e/H_d	H_e (m)	H_o (m)	H_v (m)	Modeling time (sec)	Remarks
PR00, PR05, PR30	1	0.50	5.000	4.940	0.060	50.00	Prototype
	2	1.00	10.000	9.610	0.390		
	3	1.33	13.300	12.500	0.800		
M50	1	0.50	0.100	0.099	0.001	7.07	1/50 Model
	2	1.00	0.200	0.192	0.008		
	3	1.33	0.266	0.250	0.016		
M100	1	0.50	0.050	0.049	0.001	5.00	1/100 Model
	2	1.00	0.100	0.096	0.004		
	3	1.33	0.133	0.125	0.008		
M200	1	0.50	0.025	0.025	0.000	3.53	1/200 Model
	2	1.00	0.050	0.048	0.002		
	3	1.33	0.067	0.063	0.004		

normal velocities. Typically, these boundary conditions are set using so called "wall functions." That is, it is assumed that a logarithmic velocity profile exists near a wall, which can be used to compute an effective shear stress at the wall. Wall shear stresses are thereby applied to the weir surface using local Reynolds numbers and a algorithm taking into account the available fractional flow area (Flow Science, 2002).

The upstream boundary condition can be computed with one of two pressure boundary conditions, static and stagnation. For the hydrostatic stagnation condition, $p_{bcs} = H_e$ with $u = 0$, and for the static condition, $p_{bc} = H_o$ with $u \neq 0$. In some applications, the approach velocity may not be significant and therefore omitted. However, the approach velocity is significant at the higher flows. In this study, hydrostatic stagnation condition is used. Eq. (2) and energy equation are used to determine the upstream elevation head and approach velocity head. Upstream boundary conditions which are not considered energy loss due to wall frictions are summarized following Table 2. In this study, 10 m is adopted as the design head of prototype.

4. Results

4.1. Discharge Flowrate over Ogee-Spillway

Unit discharge flowrate over the spillway for several roughness heights is summarized in Table 3. The discharge flowrates on the prototype are investigated with several surface roughness heights of the solid obstacle, i.e., approach channel and ogee-spillway. Since the roughness height of concrete is about 0.1 to 3.0 mm

Table 3. Unit Discharge Flowrate Over Ogee-Spillway for Several Surface Roughness Height

H_e/H_d	Eq. (2)		Modeling results (m^3/sec/m)		
	C	q (m^3/sec/m)	PR00	PR05	PR30
0.5	1.991050	22.261	22.677	22.631	22.579
1.0	2.164175	68.437	70.086	69.950	69.8104
1.33	2.251864	109.224	111.481	111.256	111.059

according to Table 1, numerical modelings in which surface roughness height are hydraulically smooth, k = 0.5 mm, and k = 3 mm are carried out and the results are investigated. The results of the stage-discharge relation, Eq. (2) are also presented for the comparison. The discharge flowrate decreases slightly with an increase of surface roughness height. The maximum reduction rate to the maximum flowrate due to the roughness is just about 0.4%. And the modeling results overestimate the results of Eq. (2) about 2.0%. If the simplicity and applicability of Eq. (2) are considered, the 2.0% difference is an evidence of the usefulness of Eq. (2).

Table 4. Unit Discharge Flowrate Over Ogee-Spillway for Several Model Scale

H_e/H_d	Eq. (2)		Modeling results (m^3/sec/m)			
	C	q (m^3/sec/m)	PR05	M50	M100	M200
0.5	1.991050	22.261	22.631	22.592	22.525	22.504
1.0	2.164175	68.437	69.950	69.698	69.630	69.522
1.33	2.251864	109.224	111.256	111.041	110.899	110.665

Unit discharge flowrate for several model scale is summarized in Table 4. Surface roughness height of the prototype is adopted as 0.5 mm which is considered as the surface roughness height of concrete. Surface roughness height of the several models was adjusted as the geometric similarity. The computational meshes of a prototype and scaled models were also adjusted as the geometric similarity to exclude a generation of different numerical errors in the different scaled meshes. The results of the stage-discharge relation, Eq. (2) are also presented in Table 4 for the comparison. Table 4 shows that the discharge flowrate decreases slightly as the length scale ratio of the model to the prototype increases. The maximum reduction rate in the 1/200 scaled model to the maximum flowrate in the prototype is just about 0.6%. This shows that the distortion of the Reynolds number due to minimizing the prototype is not important in a view point of discharge flowrate.

4.2. Water Surfaces over Ogee-Spillway

Water surfaces over ogee-spillway under three different upstream water heads are depicted in Fig. 4. The experimental results of USACE Waterways Experiment Station (WES) are also depicted for the comparison. The experimental results are applicable to standard spillway crests of high overflow dams without piers or abutment effects. Fig. 4(a) is on the modeling results for the prototype and this figure comparatively depicts the water surfaces over the spillway for hydraulically smooth surface (PR00) and surface roughness, k = 3 mm (PR30). Fig. 4(b) is on the modeling results which show water surfaces over the spillway for the prototype (PR05) and 1/200 scaled model (M200). The figures show that the range of water surface fluctuation is so little with a change of surface roughness and model scale. So, we can infer that numerical errors due to the surface roughness are insignificant if we just use a general roughness height of concrete and the scaled effects of the model are appeared in acceptable error range if the length scale ratio is less than 100 or 200 in a view point of water surfaces over the spillway.

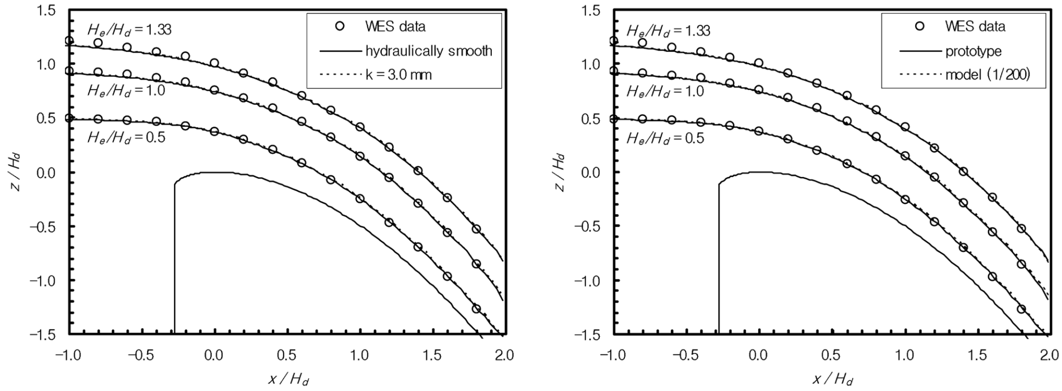

(a) with surface roughness (b) with model scale

Fig. 4. Water Surfaces over the Ogee-spillway

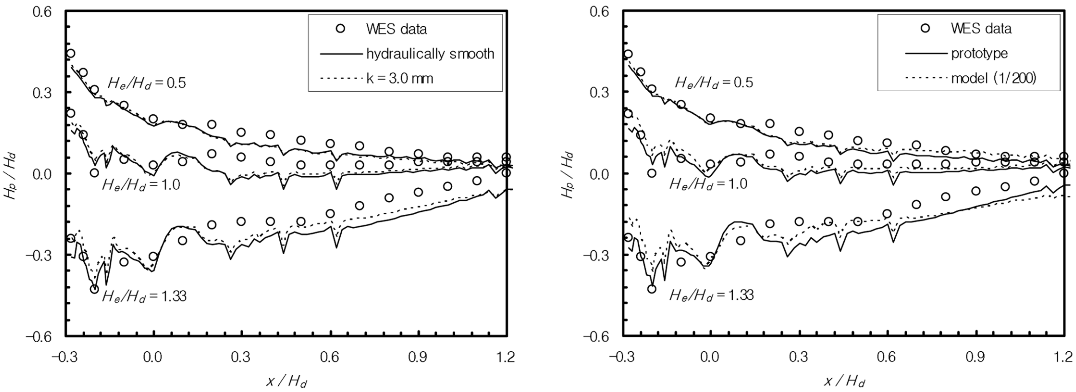

(a) with surface roughness (b) with model scale

Fig. 5. Crest Pressures on the Ogee-spillway Crest

4.3. Pressures Distributions on the Ogee-Spillway Crest

The pressure distributions on the ogee-spillway crest under three different upstream water heads are depicted in Fig. 5 in dimensionless plot in which H_p is pressure head. The experimental results of WES are also depicted for the comparison. The experimental data are applicable to high overflow dams with standard crests. Fig. 5(a) is on the modeling results for the prototype and this figure comparatively depicts the crest pressures on the spillway for hydraulically smooth surface (PR00) and surface roughness, $k = 3$ mm (PR30). Fig. 5(b) is on the modeling results which show crest pressure distributions on the spillway for the prototype (PR05) and 1/200 scaled model (M200). If the spillway profile is designed exactly in the shape of the lower nappe of a free overflow, the pressure on the spillway crest under the design head should be theoretically nil. As the spillway must be operated under heads other than the design head, the pressure will increase under the lower heads and decrease under the higher heads. The numerical results are almost identical to the theoretical pressure distributions and the experimental results. The figures show that a little crest pressure variation occurs with a change of surface roughness and model scale.

4.4. Vertical Distributions of Velocity

Vertical distributions of velocity over the ogee-spillway crest for $H_e/H_d = 1.33$ are depicted in Fig. 6 in dimensionless plot in which $V_{\max}$ is maximum velocity at any section. Fig. 6(a) is on the modeling results for the prototype and this figure comparatively depicts the vertical distributions of velocity over the spillway for hydraulically smooth surface (PR00) and surface roughness, $k = 3$ mm (PR30). The main flow characteristics of the standard ogee-spillway can be observed in this figure. The flow at the bottom layer is accelerated at first in the spillway front and the flow at the free surface is more and more accelerated passing the crest axis. Finally, the flow is evolved to the logarithmic distribution. In the lower location than the vertical location, h_m on which maximum velocity, $V_{\max}$ occurs, the velocity of the flow with smooth surface is larger than that with rough surface. In the upper, h_m the velocity of the flow with smooth surface is smaller than that with rough surface. Fig. 6(b) is on the modeling results which show the vertical distributions of velocity over the spillway for the prototype (PR05) and 1/200 scaled model (M200). Fig. 6(b) is almost similar to Fig. 6(a). If h_m is chosen as a reference point, the velocity of the prototype is larger than that of the scaled model below the reference point but the velocity of the prototype is smaller than that of the scaled model above the reference point. This phenomena occurs because the surface roughness of the scaled model is reduced as the geometric similarity but the same fluid is used in the modeling on both prototype and scaled model. That is to say, the viscosity effects increase more and more as the length scale ratio increases. The modeling results show that the scale effects give rise to similar phenomena due to the roughness effects. The roughness and scale effects are more severe below h_m than above h_m. Velocity distributions for $H_e/H_d = 1.0$ and 0.5 are depicted in Fig. 7 and

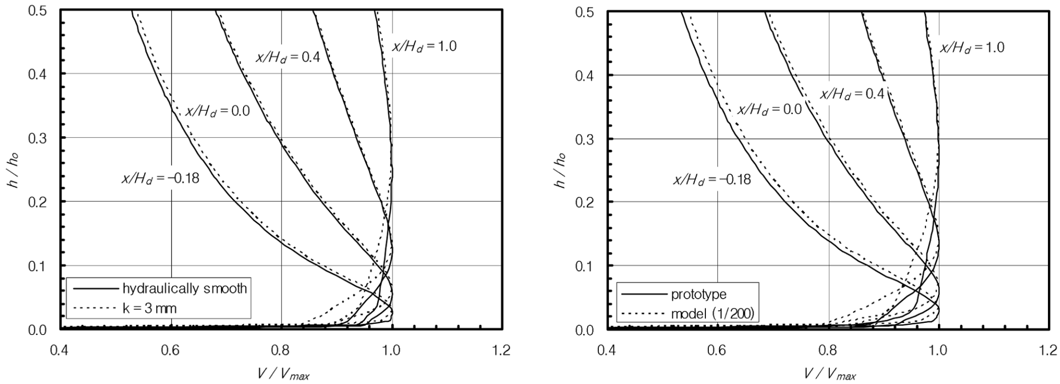

(a) with surface roughness (b) with model scale

Fig. 6. Vertical Distributions of Velocity (H_e/H_d = 1.33)

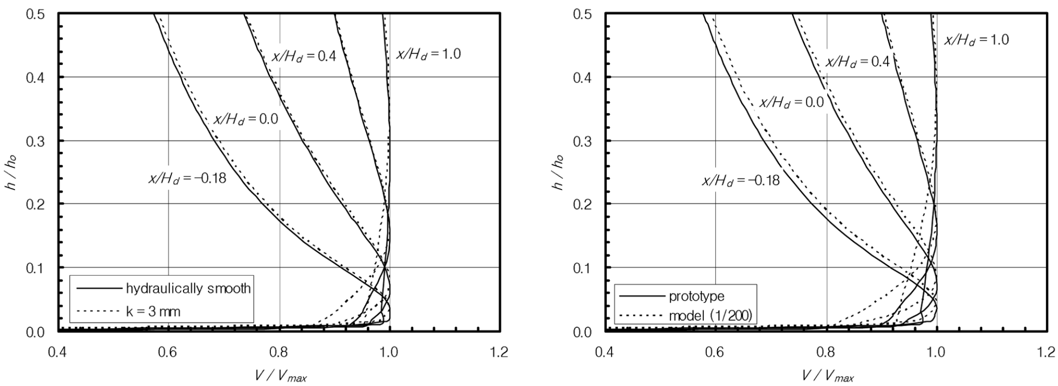

(a) with surface roughness (b) with model scale

Fig. 7. Vertical Distributions of Velocity Speed (H_e/H_d = 1.0)

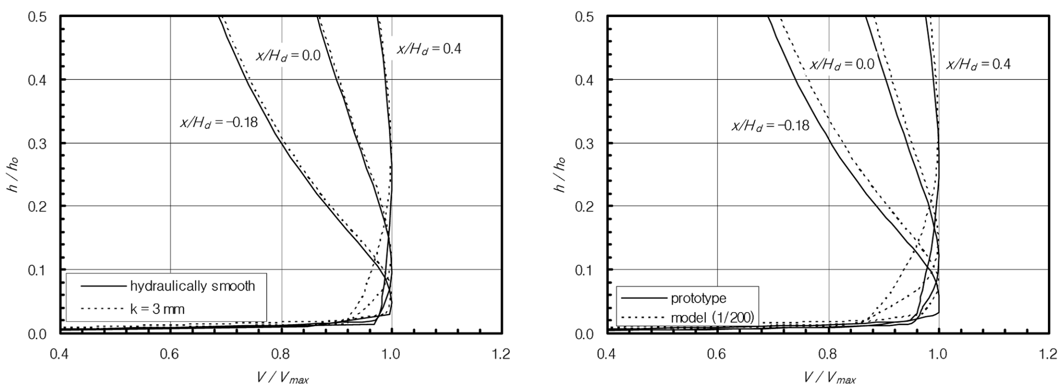

(a) with surface roughness (b) with model scale

Fig. 8. Vertical Distributions of Velocity Speed (H_e/H_d = 0.5)

Fig. 8, respectively and general tendency of the velocity distributions is almost same to Fig. 6. But after passing the crest axis, the flow is more quickly evolved to the logarithmic distribution as the upstream water heads decrease.

4.5. Vertical Distributions of Pressure Head

Vertical distributions of pressure head over the ogee-spillway crest for H_e/H_d= 1.33 are depicted in Fig. 9 in dimensionless plot. Fig. 9(a) is on the modeling results for the prototype and this figure comparatively depicts the vertical distributions of pressure head over the spillway with hydraulically smooth surface (PR00) and surface roughness, k = 3 mm (PR30). In the upstream of the crest axis, the pressure distributions are similar to the hydrostatic distributions to an extent as the flow depth increases and the pressure is quickly reduced to a negative pressure as the flow depth approaches to h_o. In the downstream of the crest axis, as the pressure approaches to an atmospheric pressure on the spillway crest, the pressure distributions are almost uniform to the atmospheric pressure at all depth. The negative pressure somewhat increases as the surface roughness of the spillway becomes smooth but the pressure distributions are almost same regardless of the surface roughness. Fig. 9(b) is on the modeling results which show the pressure distributions over the spillway for the prototype (PR05) and 1/200 scaled model (M200) and the

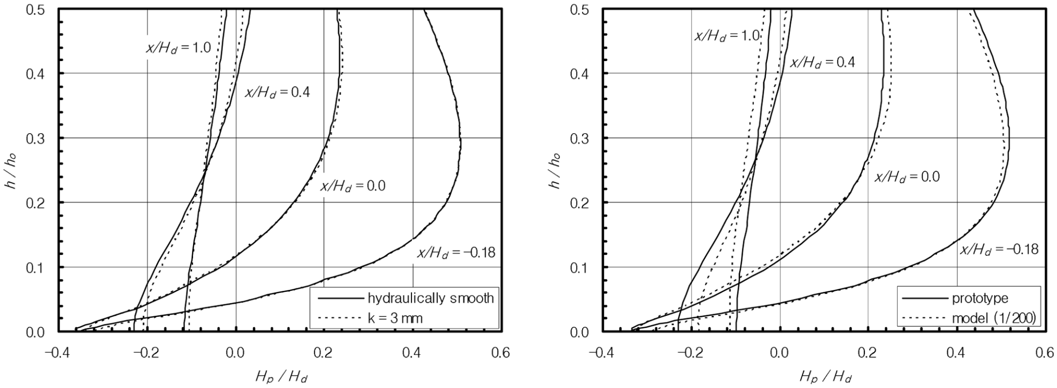

(a) with surface roughness (b) with model scale

Fig. 9. Vertical Distributions of Pressure Head (H_e/H_d = 1.33)

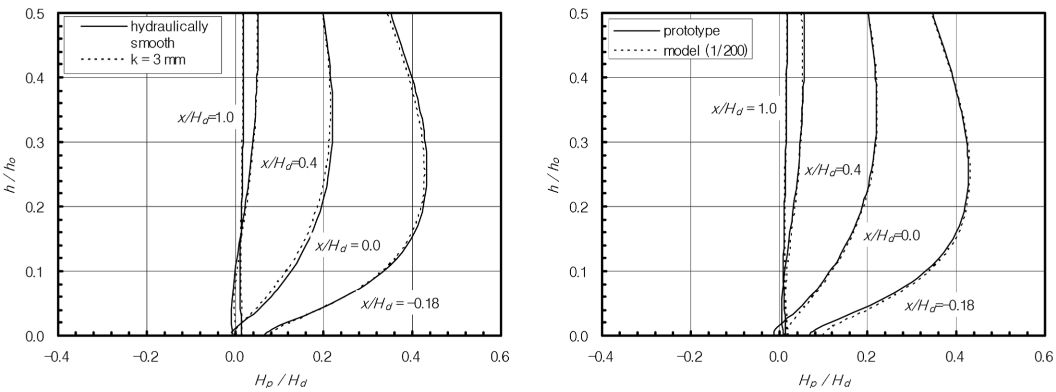

(a) with surface roughness (b) with model scale

Fig. 10. Vertical Distributions of Pressure Head (H_e/H_d = 1.0)

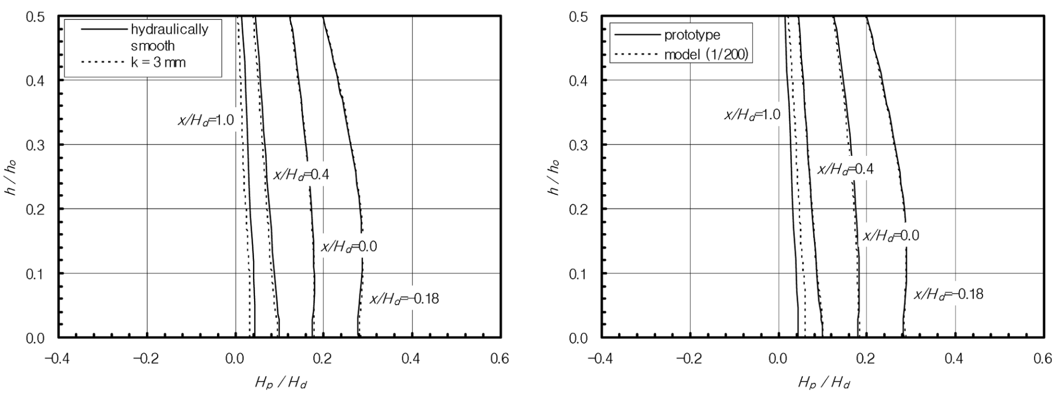

(a) with surface roughness (b) with model scale

Fig. 11. Vertical Distributions of Pressure Head (H_e/H_d= 0.5)

results are almost same to Fig. 9(a). The pressures on the spillway crest are somewhat different with a change of the surface roughness and model scale. But the pressure distributions are almost the same for each other regardless of the surface roughness and model scale. The pressure distributions for H_e/H_d= 1.0 and 0.5 are depicted in Fig. 10 and Fig. 11, respectively and general tendency of the pressure distributions is almost same to Fig. 9.

4.6. Maximum Velocity and Its Vertical Location

Maximum velocity and its vertical location at any section are investigated by using the vertical distributions of velocity in section 4.4. The maximum velocity at any section along x-axis is depicted in Fig. 12. Fig. 12(a) is on the modeling results for the prototype and this figure comparatively depicts the maximum velocity with hydraulically smooth surface (PR00) and surface roughness, k = 3 mm (PR30). Maximum velocity is slightly decreasing as the surface roughness increases. As the upstream water head increases, the reduction rate of the maximum velocity also increases, that is to say, the effects of the surface roughness increase. Fig. 12(b) is on the modeling results which show the maximum velocity distributions along x-axis for the prototype (PR05) and 1/200 scaled model (M200). The maximum velocity

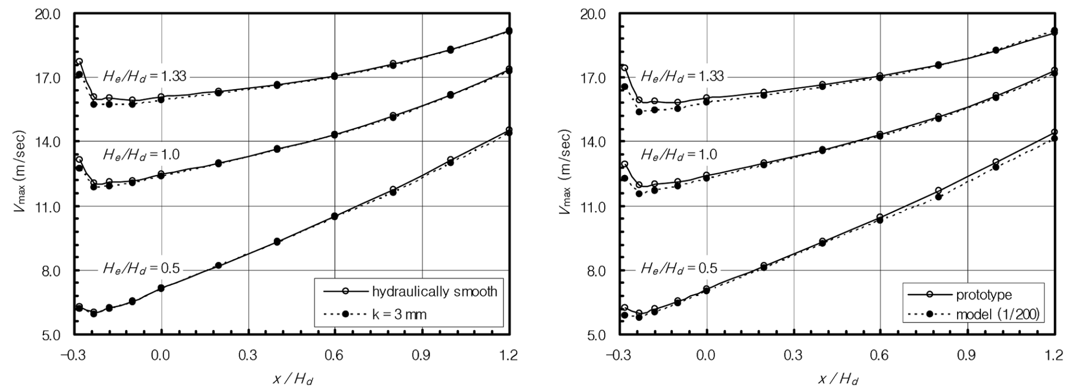

(a) with surface roughness (b) with model scale

Fig. 12. Maximum Velocity Distributions

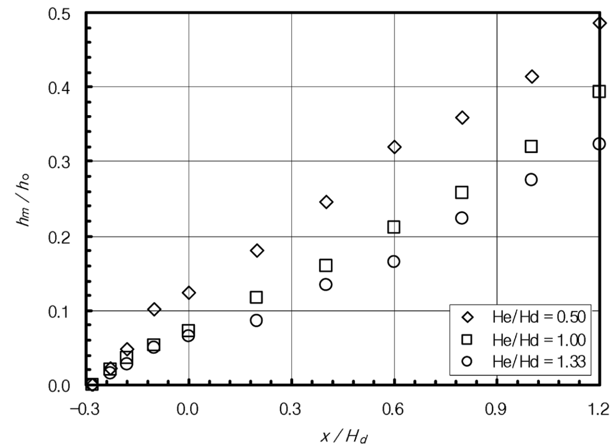

Fig. 13. Vertical Locations on which the Maximum Velocity Occurs

on the scaled model is less than that on the prototype because the scale effects give rise to similar phenomena due to the roughness effects as pointed out above section 4.4. Vertical locations on which the maximum velocity occurs for H_e/H_d = 0.5, 1.0, and 1.33 are depicted in Fig. 13 in dimensionless plot. The vertical location is relative to the location of the entire water depth, h_o. Fig. 13 shows that the vertical location where maximum velocity occurs is located on lower position as the upstream water head increases and the location is almost linearly increasing with the distance from the spillway front.

5. Conclusions

In this study, flow characteristics such as flowrate, water surfaces, crest pressures on the ogee-spillway, and vertical distributions of velocity and pressure in consideration of model scale and surface roughness effects are investigated in detail by using commercial CFD model, FLOW-3D which is widely verified and used in the field of spillway flow analysis. To investigate the scaling and roughness effects, six cases are adopted. Namely, numerical modeling on the hydraulically smooth (PR00), k = 0.5 mm (PR05), and k = 3.0 mm (PR30) for the investigation of roughness effects and prototype (PR05), 1/50 model (M50), 1/00 model (M100), 1/200 model (M200) for the investigation of scale effects are carried out. In the modeling of the scaled model, grid resolution, surface roughness, and upstream boundary conditions were adjusted as the geometric similarity to exclude a generation of different numerical error.

The important simulation results comprise the following: 1) The discharge flowrate decreases slightly as surface roughness height and the length scale of the model to the prototype increase. The water surface fluctuation is negligible and some crest pressure variation occurs with a change of surface roughness and model scale. Numerical errors due to the surface roughness are insignificant if we just use a general roughness height of construction materials and the scale effects of the model are appeared in within an acceptable error range if the length scale ratio is less than 100 or 200. 2) The modeling results show that increasing of the length scale ratio give rise to similar phenomena due to increasing of the surface roughness. If h_m is chosen as a reference point, the velocity of the prototype is larger than that of the scaled model below the reference point but the velocity of the prototype is smaller than that of the scaled model above the reference point. The roughness and scale effects are more severe below the reference point. 3) The pressures on the spillway crest are somewhat different with a change of the surface roughness and model scale. But the vertical pressure distributions are almost same to each other regardless of the surface roughness and model scale. 4) Maximum velocity at any section is slightly decreasing as the surface roughness and the length scale ratio increase. The vertical location on which maximum velocity occurs is located on lower position as the upstream water head increase and the location is almost linearly increasing with the distance from the spillway front.

References

ASCE Task Committee on Hydraulic Modeling (2000). *Hydraulic modeling: concepts and practice*, ASCE Publications, Reston, VA.

Assy, T. (2000). "Solution for spillway flow by finite difference method." *J. of Hydraulic Research.*, IAHR, Vol. 39, No. 3, pp. 241-247.

Betts, P.L. (1979). "A variation principle in terms of stream function for free surface flows and its application to finite element method." *Comp. and Fluids*, Vol. 7, No. 2, pp. 145-153.

Bureau of Reclamation, US Department of the Interior (1980). *Hydraulic laboratory techniques*, Bureau of Reclamation, Denver, Colorado.

Cassidy, J.J. (1965). "Irrotational flow over spillways of finite height." *J.*

of Engrg. Mech. Div., ASCE, Vol. 91, No. 6, pp. 155-173.
Flow Science (2002). *FLOW-3D. [Theory manual]*. Los Alamos, NM.
Guo, Y., Wen, X., Wu, C., and Fang, D. (1998). "Numerical modeling of spillway flow with free drop and initially unknown discharge." *J. of Hydraulic Research.*, IAHR, Vol. 36, No. 5, pp. 785-801.
Hager, W.H. (1999). *Wastewater hydraulics*, Springer-Verlag, Berlin, Heidelberg, Germany.
Ho, D.K.H. and Donohoo, S.M. (2001). "Investigation of spillway behavior under increased maximum flood by computational fluid dynamics technique." *Proc. 14th Australasian Fluid Mech. Conference*, Adelaide University, Adelaide, Australia, pp. 10-14.
Ikegawa, M. and Washizu, K. (1973). "Finite element method applied to analysis of flow over a spillway crest." *Int. J. of Numerical Methods in Engrg.*, Vol. 6, pp. 179-189.
Kim, N.I. (2003). *Investigation of scale effects of hydraulic model for dam spillway using 3-D CFD model*, [Dissertation], Dept. of Civil Engineering, Seoul National University, Seoul, Korea.
Li, W., Xie, Q., and Chen, C.J. (1989). "Finite analytic solution of flow over spillways." *J. of Engrg. Mech.*, ASCE, Vol. 115, No. 12, pp. 2635-2648.
Olsen, N.R. and Kjellesvig, H.M. (1998). "Three-dimensional numerical flow modeling for estimation of spillway capacity." *J. of Hydraulic Research*, IAHR, Vol. 36, No. 5, pp. 775-784.
Savage, B.M. and Johnson, M.C. (2001). "Flow over ogee spillway: Physical and numerical model case study." *J. of Hydraulic Engrg.*, ASCE, Vol. 127, No. 8, pp. 640-649.
Song, C.C.S. and Zhou, F. (1999). "Simulation of free surface flow over spillway." *J. of Hydraulic Engrg.*, ASCE, Vol. 125, No. 9, pp. 959-967.
Unami, K., Kawachi, T., Babar, M.M., and Itagaki, H. (1999). "Two-dimensional numerical model of spillway flow." *J. of Hydraulic Engrg.*, ASCE, Vol. 125, No. 4, pp. 369-375.
US Army Corps of Engineers (USACE) (1988). *Hydraulic design criteria*, Mississippi, USA.
US Bureau of Reclamation (USBR) (1973). *Design of small dams*, Washington, USA.
Yakhot, V., Orsarg, S.A., Thangam, S., Gatski, T.B., and Speziale, C.G. (1992). "Development of turbulence models for shear flows by a double expansion technique." *Physics of Fluids*, Vol. 4, No. 7, pp. 1510-1520.

(Received on June 1, 2004 / Accepted on August 17, 2004)